LBL-2764 c.2

Presented at the ASTM Symposium on Properties of Materials for Liquid Natural Gas Tankage, Boston, Mass., May 21-22, 1974.

LAWRENCE RADIATION LABORATORY
JUL 30 1974
LIBRARY AND DOCUMENTS SECTION

THE CRYOGENIC PROPERTIES OF Fe-Mn AND Fe-Mn-Cr ALLOYS

M. J. Schanfein, M. J. Yokota, V. F. Zackay, E. R. Parker and J. W. Morris, Jr.

May 1974

Prepared for the U. S. Atomic Energy Commission under Contract W-7405-ENG-48

TWO-WEEK LOAN COPY

This is a Library Circulating Copy which may be borrowed for two weeks. For a personal retention copy, call Tech. Info. Division, Ext. 5545

LAWRENCE BERKELEY LABORATORY
UNIVERSITY OF CALIFORNIA
BERKELEY

LBL-2764 c.2

DISCLAIMER

This document was prepared as an account of work sponsored by the United States Government. While this document is believed to contain correct information, neither the United States Government nor any agency thereof, nor the Regents of the University of California, nor any of their employees, makes any warranty, express or implied, or assumes any legal responsibility for the accuracy, completeness, or usefulness of any information, apparatus, product, or process disclosed, or represents that its use would not infringe privately owned rights. Reference herein to any specific commercial product, process, or service by its trade name, trademark, manufacturer, or otherwise, does not necessarily constitute or imply its endorsement, recommendation, or favoring by the United States Government or any agency thereof, or the Regents of the University of California. The views and opinions of authors expressed herein do not necessarily state or reflect those of the United States Government or any agency thereof or the Regents of the University of California.

THE CRYOGENIC PROPERTIES OF Fe-Mn and Fe-Mn-Cr ALLOYS

M. J. Schanfein, M. J. Yokota, V. F. Zackay,
E. R. Parker and J. W. Morris, Jr.

Inorganic Materials Research Division, Lawrence Berkeley Laboratory and
Department of Materials Science and Engineering, College of Engineering;
University of California, Berkeley, California 94720

ABSTRACT: A wide range of microstructures were obtained in Fe-Mn alloys by varying the manganese and chromium contents. When a bcc (α) structure was produced, increasing amounts of manganese were found to be detrimental to low temperature toughness. At manganese levels greater than 12% where appreciable amounts of ϵ and γ phases formed the ductile-brittle transition temperature dropped rapidly. In terms of the ($\epsilon + \gamma$) phases present, the ductile-brittle transition temperature decreased at a rate of 1.3°C/vol% ($\epsilon + \gamma$). Increasing the ($\epsilon + \gamma$) content to achieve good low temperature toughness, however, also caused a decrease in the yield strength. Increases in the yield strength were achieved without appreciable increase in the ductile-brittle transition temperature by greater manganese additions and by chromium additions.

KEY WORDS: fracture (toughness), ductile-brittle transition, mechanical properties, microstructure.

Introduction

If superior iron-base cryogenic alloys are to be developed to meet the ever-increasing demands of technology it is necessary to understand the atomistic and microstructural roles of the common alloying elements of iron at low temperatures. In this paper, the preliminary results of a study of the influence of the element manganese on the cryogenic properties of iron are reported. The properties of several Fe-Mn alloys were compared to those of the cryogenic Fe-Ni-Ti alloys developed in the authors' laboratory in the last several years [1-3].

The beneficial effect of nickel in lowering the ductile-brittle transition temperature (DBTT) of iron-carbon alloys [4] has been known since the 1940's. The knowledge of this phenomenon has led to the development of an entire class of commercial cryogenic alloys. Recently it was shown that Ni lowers the DBTT of carbon free iron as well [5,6]. The atomistic and microstructural mechanisms responsible for the improvement in notch toughness resulting from nickel additions are not well understood. It is usually assumed, however, that the crystal lattice (rather than the microstructure) is influenced by the nickel solute and that the effect of nickel is to raise the cleavage strength of iron. Manganese is another solute thought to improve the low temperature ductility of iron but apparently behaves in a different way than Ni does. Jolley [5] has reported that manganese improves the notch impact properties of iron only when carbon is present. He found no improvement in the toughness of decarburized iron alloys, and concluded that the effectiveness of manganese was primarily through alteration of the morphology and distribution

of carbides. Roberts [7], in a later study of Fe-Mn alloys containing up to 9%Mn, found that the impact toughness and DBTT were relatively insensitive to the manganese content. Instead, he suggested that manganese influenced the transformation substructure and grain size. The grain size dependence of the DBTT amounted to 6-7°C/mm$^{-1/2}$ which is roughly the same grain size dependence Leslie [8] and Sasaki, et al [9] have found for Fe-Ni alloys.

In the Fe-Mn system, a variety of substructure changes occur in the bcc lattice, as shown by Roberts [7]. Additionally, when manganese contents exceed about 10%, austenitized and quenched alloys exhibit a hexagonal ϵ (Gk epsilon) phase and mixed $\alpha' + \epsilon$ (Gk alpha) microstructures result [10,11]. When the manganese content is increased beyond 15% the face centered cubic γ (Gk gamma) phase is resistant to transformation even when cooled to liquid nitrogen temperatures, and mixed $\alpha + \epsilon + \gamma$ microstructures are obtained. The cryogenic mechanical properties of such mixed microstructures have not been reported in detail in the published literature and are the subject of a continuing study in the authors' laboratory.

The DBTT phenomenon is normally associated with alloys having a bcc or bct crystal structure. Alloys with these crystal structures usually have adequate strength but are limited by a tendency toward catastrophic failure at low temperatures. Hexagonal, and especially fcc structures, normally do not possess a DBTT except in certain cases where solute or precipitate segregation at grain boundaries occurs [12]. The strength of alloys with the hexagonal or fcc crystal structure is generally lower than those with the bcc structure, although the low temperature ductility is

good. A primary objective of the present study was to explore the feasibility of designing Fe-Mn alloys with mixed microstructures for attaining combinations of strength and toughness which are equal to or superior to those of the cryogenic Fe-Ni alloys.

Recent studies in this laboratory and elsewhere [13-15] have shown that strain induced transformations can significantly raise the ductility and fracture toughness of alloys having metastable matrices. In the Fe-Mn system, the possible strain induced transformations are those of the hexagonal ϵ phase transforming during deformation to bcc α and of the retained austenite transforming to either ϵ or α, or both. White and Honeycombe [10], and more recently Holden, et al [11], found phase transformations of this kind to occur during cold working of Fe-Mn alloys whose compositions were similar to those of the present study.

Materials and Experimental Procedure

The compositions and designations of the Fe-Mn alloys used in the present investigation are listed in Table 1. All alloys contained 0.10%Ti and 0.05%Al which were added to immobilize the interstitials carbon, nitrogen and oxygen. The C+N+O content of the alloys was about 0.02%. Alloys were induction melted in an inert atmosphere and cast into three inch diameter ingots in copper chill molds. The ingots were vacuum homogenized for 24 hours at 1200°C, furnace cooled, reheated to 1200°C, and then upset forged and air cooled.

Charpy and tensile specimen blanks were austenitized at 900°C for 2 hrs, ice-brine quenched and then cooled to liquid nitrogen temperature (-196°C). The prior austenite grain sizes of all alloys were in the

range 30-50 μ. Sheet tensile specimens 0.15 in. thick, a gage section width of 0.125 in. and a gage length of 1.0 in., and standard Charpy V-notch impact specimens were carefully machined from the heat treated blanks.

Impact tests were carried out (in accordance with ASTM procedure E-23-64) on a 225 ft.lb^e capacity impact testing machine. Liquid helium, liquid nitrogen, isopentane, and methyl alcohol-dry ice mixtures were used as cryogenic coolants. Tensile tests were performed on a 11,000 lb capacity Instron testing machine using a crosshead speed of 0.1 cm/min. Yield strength was determined by the 0.2% offset method.

The kinetics of the phase transformations during both heating and cooling were studied by dilatometry with heating and cooling rates of 10°C/min. Dilatometric measurements were made on cylindrical tubular specimens 1.0 in. long, 0.25 in. in outside diameter and with a 0.10 in. internal diameter.

Quantitative measurements of the amount and type of phases present were made using a Picker X-ray diffractometer with a Cu K_α source and an LiF monochromator between the diffracted beam and detector. The percentages of the phases present were determined by comparing the integrated diffraction intensities of the (200) and (211) diffraction peaks of the α phase, the (220) peak of the γ phase, and (012) and (013) peaks of the ϵ phase. The surfaces of X-ray and metallographic specimens were carefully prepared so as to avoid changes in structure from mechanically induced transformation. Specimens were chemically etched in Klemm's reagent with acetic acid.

Fracture surfaces of broken Charpy specimens were examined in a Jeolco JSM-U3 scanning electron microscope with the secondary emission operated at 25kV.

Results and Discussion

The phase transformation temperatures of Fe-Mn alloys as determined by dilatometry are shown in Fig. 1. Also shown in Fig. 1 are the results of other investigators [11,16]. When these alloys were cooled from the austenite phase a variety of complex microstructures resulted. The as-quenched structure of low manganese alloys which were cooled to LN (-196°C) was entirely bcc. However, it has been reported [7] that the substructure morphology changes from equiaxed ferrite (α) to lath and plate martensites (α') as the manganese content is increased to about 12%. In Fig. 2 are shown micrographs illustrating the structure of the Fe-Mn alloys of the present study. An example of the typical lath martensite microstructure of the 12%Mn alloy is shown in Fig. 2(a). In alloys with manganese contents greater than 12% increasing amounts of the hexagonal ϵ phase formed. It has been reported that in alloys with approximately 30%Mn the austenite (γ) phase is completely retained even on cooling to -196°C[11]. Within the 12%-30%Mn composition range various complex microstructures, consisting of mixtures of the α', ϵ and γ phases, were obtained. Examples of these mixed microstructures are shown in Figs. 2(b) and 2(c). The microstructure of the 16%Mn alloy (Fig. 2(b)) was predominantly $\alpha' + \epsilon$ while that of the 20%Mn alloy was entirely $\epsilon + \gamma$ (Fig. 2(c)).

The sequence of structural changes in Fe-Mn alloys was similar to that in the more familiar Fe-Ni system, except for the occurrence, in Fe-Mn alloys, of the hexagonal ϵ phase. This phase has been found only in those alloy systems where solute additions decrease the stacking fault energy of the austenite to very low values approaching zero. At these very low stacking fault energies the driving force necessary for the $\gamma \rightarrow \epsilon$ transformation is reduced below that of the $\gamma \rightarrow \alpha'$ transformation and a metastable ϵ phase forms [17].

The Charpy impact toughness for the various Fe-Mn alloys of the present investigation is plotted as a function of temperature in Fig. 3. The fracture surfaces of the Charpy bars broken at both room (25°C) and LN (-196°C) temperatures are shown in Fig. 4, and correspond to the microstructures illusrated in Fig. 2. The room temperature Charpy fractures of the 12%Mn, 16%Mn and 20%Mn alloys revealed dimpled rupture characteristic of ductile behavior. In liquid nitrogen (-196°C) tests, the 12%Mn alloy exhibited features due to intergranular failure while the 16%Mn and 20%Mn alloys showed predominantly dimpled rupture with some quasi-cleavage.

In Fig. 5 is shown a plot relating the DBTT to manganese content. It is evident from Fig. 5 that as the manganese content increased the DBTT first increased up to approximately 8%Mn and then decreased rapidly at a rate of 21°C/at.%Mn. Also shown in Fig. 5 is the DBTT behavior of interstitial-free Fe-Ni alloys which exhibited a DBTT decrease at the rate of 15%C/at.%Ni [6].

It was established from X-ray phase analysis, Table 2, that the 4%Mn and 8%Mn alloys were completely bcc while the 12%Mn, 16%Mn and 20%Mn alloys contained increasing amounts of the ϵ and γ phases. The 16%Mn alloy had an $\alpha + \epsilon + \gamma$ mixed microstructure while the 20%Mn alloy had an $\epsilon + \gamma$ mixed microstructure. Thus the results of the X-ray analysis and DBTT determinations suggested that the ϵ or γ or both phases were responsible for the improved low temperature toughness of the higher manganese alloys (12 to 20%Mn). The variation of the DBTT as influenced by the amount of ϵ phase present is shown in Fig. 6. The decrease in the DBTT was approximately 3°C per volume percent ϵ. In terms of the total volume percent of the ϵ and γ phases, the decrease in DBTT was 1.3°C per volume percent ($\epsilon + \gamma$). Alternatively, this decrease in DBTT could be attributed to a decrease in the volume percentage of α present.

It was evident that the relation between microstructure and cryogenic mechanical properties for the Fe-Mn alloys of the present study was quite different from that for the interstitial-free Fe-Ni alloys. The Fe-Ni alloys exhibited a decrease in the DBTT with increasing nickel content in a single phase bcc structure. In the Fe-Ni system, as previously mentioned, the lowering of the DBTT by nickel is essentially due to solute-lattice interaction rather than due to a microstructural effect, while in Fe-Mn alloys the decrease in DBTT was accompanied by microstructural changes involving variations in the relative amounts of the α, ϵ, and γ phases.

Besides a low DBTT, an adequate yield strength must also be developed in an alloy which is to be considered for cryogenic applications. The

yield and ultimate tensile strengths, both at room and LN temperature, for alloys of the present investigation are plotted as a function of manganese content in Fig. 7. Similar plots for elongation and reduction in area are shown in Fig. 8. From these figures it can be seen that the 4%Mn, 8%Mn and 12%Mn alloys with bcc matrices exhibited fairly high yield strength but rather poor elongation. As the manganese content of the alloys was increased, the amount of the hexagonal ϵ phase also increased. This in turn led to a considerable decrease in yield strength. The room temperature yield strength of the 16%Mn alloy which had almost 50% ϵ was only 30 ksi. Increase in the manganese content to 20% resulted in stabilization of the γ phase, and no α phase was present in the as-quenched alloy. The alloy contained 66% ϵ and 34% γ. It was surprising that although a stronger phase, α, was replaced by a weaker phase, γ, both the yield strength and elongation increased. At room and LN temperatures yield strengths of 60 and 78 ksi respectively, and elongations of 43 and 62% respectively, were obtained for the 20%Mn alloy. Thus it appeared that with increasing amounts of ϵ in a primarily α microstructure the yield strength decreased; however, when the microstructure was predominantly ϵ, and γ replaced α, the yield strength increased.

The above behavior can be rationalized if account is taken of the differences in yield strengths between phases and the changing stability of the ϵ phase with increasing manganese content. In an $\alpha + \epsilon$ duplex structure, the flow or strain tends to concentrate in the weaker ϵ phase, and the yield strength is controlled by the strength of the ϵ phase. The results of X-ray analysis (Table 2) clearly indicated that during

tensile testing the ϵ phase in the 16%Mn alloy transformed to α. It was probable that a stress induced martensitic transformation of ϵ to α contributed to the low yield strength of the 16%Mn alloy. Stress induced transformations have been reported in several metastable austenitic steels of low austenite stability [15,18]. The increase in manganese content to 20% apparently resulted in two changes. First, it led to the elimination of the α phase and the formation of the γ phase. As a result the alloy consisted of a mixture of ϵ and γ phases of apparently comparable strengths, thus preventing localized flow in either phase. Second, the ϵ phase in the 20%Mn alloy was more stable than that in the 16%Mn alloy, thus minimizing the possibility of occurrence of a stress induced transformation. The higher stability of the 20%Mn alloy compared to that of the 16%Mn alloy was evident from the observation that during tensile testing a greater volume fraction of ϵ transformed to α in the latter alloy (see Table 2).

The inter-relationships between the DBTT and the tensile properties are shown in Fig. 9. The figure shows that the yield strength and the DBTT varied in a complex manner with increase in the manganese content. An important feature of the plot is in the region beyond 12%Mn where the hexagonal ϵ phase begins to form and the DBTT of the alloys begins to decrease rapidly. Unfortunately, it is in this range of compositions that the alloys begin to lose their strength considerably. The cause of this decrease was discussed earlier.

The relationship between microstructure, strength and toughness was also examined in several Fe-Mn alloys containing 8%Cr. In Fig. 9 are

shown plots relating strength and DBTT for these alloys. The relative proportions of the α, ϵ and γ phases in the chromium-containing alloys before and after tensile testing are indicated in Table 2. The results suggested that chromium additions to Fe-Mn alloys favored the formation of the α phase. In the as-quenched condition, the volume fraction of the α phase in the 16%Mn8%Cr alloy was almost twice that in the 16%Mn alloy. The yield strength of the chromium-containing alloy was correspondingly higher. In spite of the greater volume fraction of α (and the smaller volume fraction of ϵ) and the higher yield strength, the chromium containing alloy had approximately the same DBTT as the alloy without chromium. The reasons for this behavior are not well understood. Nevertheless, it was evident that the 8% chromium addition to the 16%Mn alloy was considerably beneficial for attaining a superior combination of strength and toughness. These properties coupled with the enhanced corrosion resistance of the 16%Mn8%Cr alloy would be very desirable in cryogenic applications. Additional decrease in the DBTT was observed with little loss in strength in the 20%Mn8%Cr alloy. The DBTT was below -196°C, the temperature of liquid nitrogen (see Fig. 9). It was interesting to note that the 20%Mn and the 20%Mn 8%Cr alloys had approximately the same strength and toughness (DBTT).

Conclusions

(1) A wide range of microstructures was produced in Fe-Mn alloys by varying the manganese and chromium contents.

(2) In alloys that contained predominantly the bcc α phase, manganese additions raised the ductile-brittle transition temperature (DBTT).

In Fe-Mn alloys without chromium, the formation of the hexagonal ϵ phase and the fcc γ phase at manganese concentrations exceeding 12% resulted in a decrease in the DBTT.

(3) The yield strength decreased with increasing amount of ϵ in a mixed $\alpha + \epsilon$ microstructure. The decrease was possibly due to localized flow in the weaker ϵ phase and a stress induced transformation of ϵ to α. The yield strength was raised when the manganese content was increased to 20%, resulting in a mixed $\epsilon + \gamma$ microstructure.

(4) Chromium additions of 8% led to increase in the yield strength of the Fe-Mn alloys without causing appreciable changes in the DBTT. In the case of the 16%Mn alloy, an 8%Cr addition nearly doubled the yield strength at approximately the same DBTT. Chromium additions did not significantly change the yield strength and the DBTT of the 20%Mn alloy. However, the enhanced oxidation resistance that would be obtained with chromium additions is considered desirable for potential cryogenic applications.

Acknowledgements

We are indebted to Dr. M. D. Bhandarkar for his critical technical review and helpful discussions.

This research was performed partially under the auspices of the U.S. Atomic Energy Commission through the Inorganic Materials Research Division of the Lawrence Berkeley Laboratory, and partially under the auspices of the National Aeronautics and Space Administration.

References

[1] Zackay, V. F., Microstructure and Design of Alloys, Institute of Metals, London, 1973, pp 591.

[2] Jin, S., Morris, J. W., Jr., and Zackay, V. F., Advances in Cryogenic Engineering, In press.

[3] Yokota, M. J., Sasaki, G., Horwood, W. A., Zackay, V. F., and Parker, E. R., In preparation.

[4] Brophy, G. R. and Miller, A. J., Transaction of the American Society for Metals, Vol. 41, 1949, pp. 1185-1203.

[5] Jolley, W., Journal of the Iron and Steel Institute, Vol. 206, Feb. 1968, pp. 170-173.

[6] Yokota, M. J., Zackay, V. F., and Parker, E. R., In preparation.

[7] Roberts, M. J., Metallurgical Transactions, American Society for Metals, Vol. 1, 1970, pp. 3287-3294.

[8] Leslie, W. C., Metallurgical Transactions, American Society for Metals, Vol. 2, 1971, pp. 1989.

[9] Sasaki, G., Yokota, M. J., and Zackay, V. F., In preparation.

[10] White, C. H. and Honeycombe, R. W. R., Journal of the Iron and Steel Institute, Vol. 200, June 1962, pp. 457-466.

[11] Holden, A., Bolton, J. D., and Petty, E. R., Journal of the Iron and Steel Institute, Vol. 209, Sept. 1971, pp 721-728.

[12] Stoloff, N. S., Fracture, Vol. 6, ed. H. Liebowitz, Academic Press, New York, 1969, pp 1-81.

[13] Gerberich, W. W., Hemmings, P. L., and Zackay, V. F., Metallurgical Transactions, American Society for Metals, Vol. 2, 1971, pp 2243-2253.

[14] Antolovich, S. D. and Singh, B., Metallurgical Transactions, American Society for Metals, Vol. 2, 1971, pp 2135-2141.

[15] Bhandarkar, D., Zackay, V. F., and Parker, E. R., Metallurgical Transactions, American Society for Metals, Vol. 3, 1972, pp 2619-2631.

[16] Hansen, M., Constitution of Binary Alloys, McGraw-Hill, New York, 1958, pp 664-668.

[17] Breedis, J. F. and Kaufman, L., Metallurgical Transactions, American Society for Metals, Vol. 2, 1971, pp 2359-2371.

[18] Reed, R. P. and Guntner, C. J., Transactions of the Metallurgical Society of the American Institute of Mining and Metallurgical Engineers, Vol. 230, 1964, pp 1713-1720.

Table 1--Chemical compositions of alloys

Designation	Compositions, Wt %		
	Mn	Cr	Fe
4%Mn	4.1	-	Bal.
8%Mn	8.1	-	Bal.
12%Mn	12.2	-	Bal.
16%Mn	16.0	-	Bal.
20%Mn	19.5	-	Bal.
12%Mn8%Cr	12.2	7.7	Bal.
16%Mn8%Cr	15.8	7.9	Bal.
20%Mn8%Cr	20.2	7.9	Bal.

Table 2--Volume percents of phases in Fe-Mn and Fe-Mn-Cr alloys

Alloy Designation	Volume Percent of Phases								
	Prior to Tensile			After Tensile Testing at 25°C			After Tensile Testing at -196°C		
	α	ε	γ	α	ε	γ	α	ε	γ
4%Mn	100	-	-	100	-	-	100	-	-
8%Mn	100	-	-	100	-	-	100	-	-
12%Mn	94.1	5.9	-	100	-	-	100	-	-
16%Mn	29.7	45.1	25.2	92.0	-	8.0	95.3	-	4.7
20%Mn	-	66.1	33.9	18.3	50.7	31.0	39.3	28.7	32.0
12%Mn8%Cr	100	-	-	100	-	-	100	-	-
16%Mn8%Cr	54.3	26.6	19.1	100	-	-	100	-	-
20%Mn8%Cr	-	60.7	39.3	27.0	41.9	31.1	61.7	21.1	17.2

Figure Captions

[1] Phase transformation temperatures for Fe-Mn alloys of the present investigation. Also shown are some results of other investigations (11,16).

[2] Microstructures of the Fe-Mn alloys of the present investigation :

(a) Lath martensite typical of the 12%Mn alloy

(b) Plate martensite (α') and the ϵ phase in the 16%Mn alloy

(c) Mixed $\epsilon + \gamma$ structure of the 20%Mn alloy.

All alloys were austenitized at 900°C, ice-brine quenched and cooled to LN temperature (-196°C) prior to examination.

[3] Charpy V-notch impact toughness vs testing temperature for Fe-Mn alloys without chromium.

[4] Scanning electron fractographs of Charpy specimens:

(a) 12%Mn alloy tested at 25°C

(b) 12%Mn alloy tested at -196°C

(c) 16%Mn alloy tested at 25°C

(d) 16%Mn alloy tested at -196°C

(e) 20%Mn alloy tested at 25°C

(f) 20%Mn alloy tested at -196°C

[5] Ductile-brittle transition temperature (DBTT) vs manganese content for Fe-Mn alloys of the present investigation. Also plotted are the data of Yokota, et al [6] on DBTT vs nickel content for non-interstitial Fe-Ni alloys.

[6] Ductile-brittle transition temperature (DBTT) vs volume percent ϵ and α phases in Fe-Mn alloys of the present investigation.

[7] Plots of yield and ultimate tensile strengths at both 25°C and -196°C vs manganese content for Fe-Mn alloys of the present investigation.

[8] Plots of elongation and reduction in area at both 25°C and -196°C vs manganese content for Fe-Mn alloys of the present investigation.

[9] Plots relating yield strength, ultimate strength and ductile-brittle transition temperature (DBTT) for Fe-Mn and Fe-Mn-Cr alloys of the present investigation. Also indicated are the phases present in the several alloys.

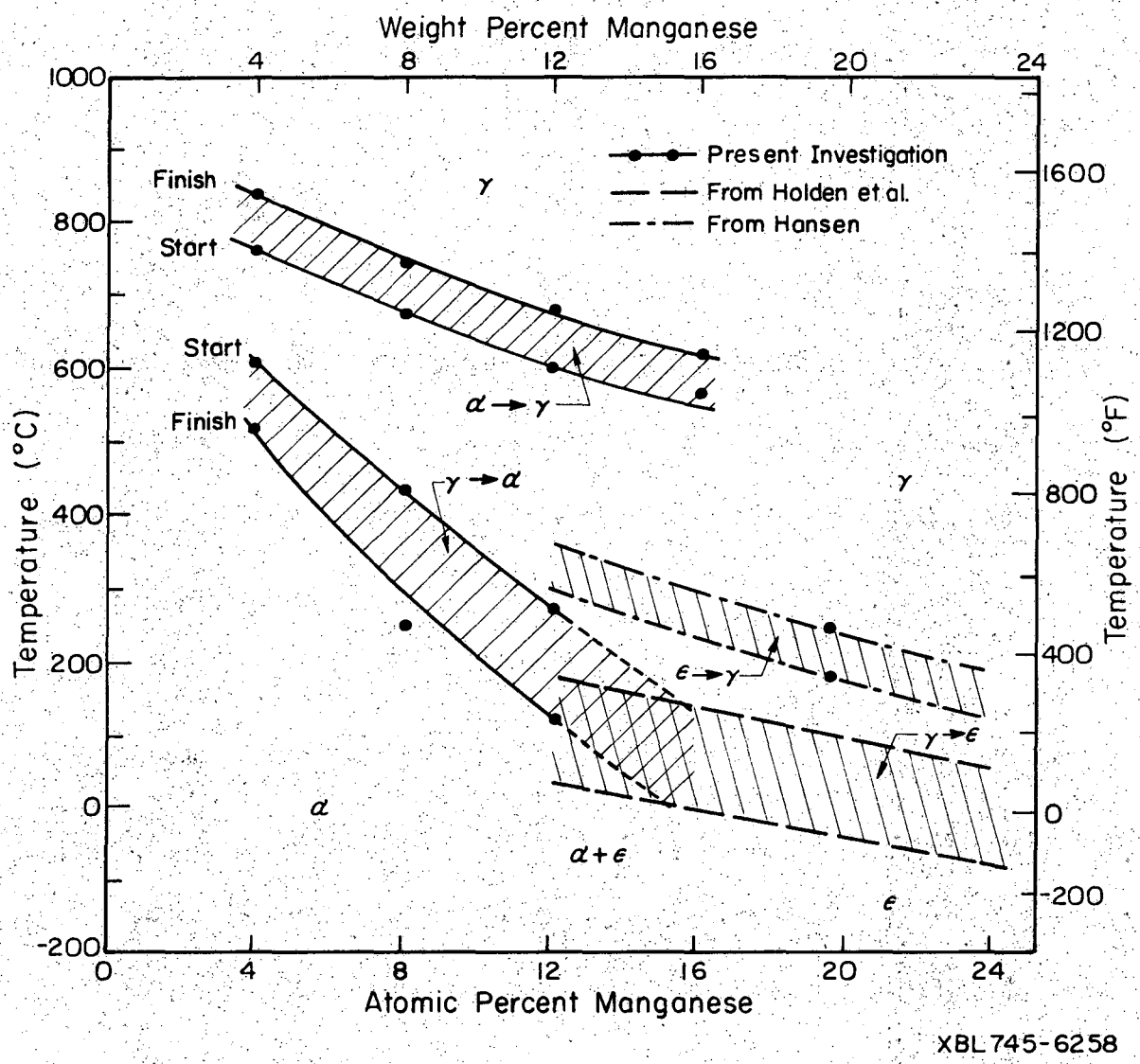
Weight Percent Manganese
4
8
12
16
20
24
1000
800
600
400
200
0
-200
Temperature (°C)
1600
1200
800
400
0
-200
Temperature (°F)
Present Investigation
From Holden et al.
From Hansen
Finish
Start
Start
Finish
γ
α → γ
γ → α
γ
ε → γ
γ → ε
α
α + ε
ε
0
4
8
12
16
20
24
Atomic Percent Manganese
XBL 745-6258

Fig. 1

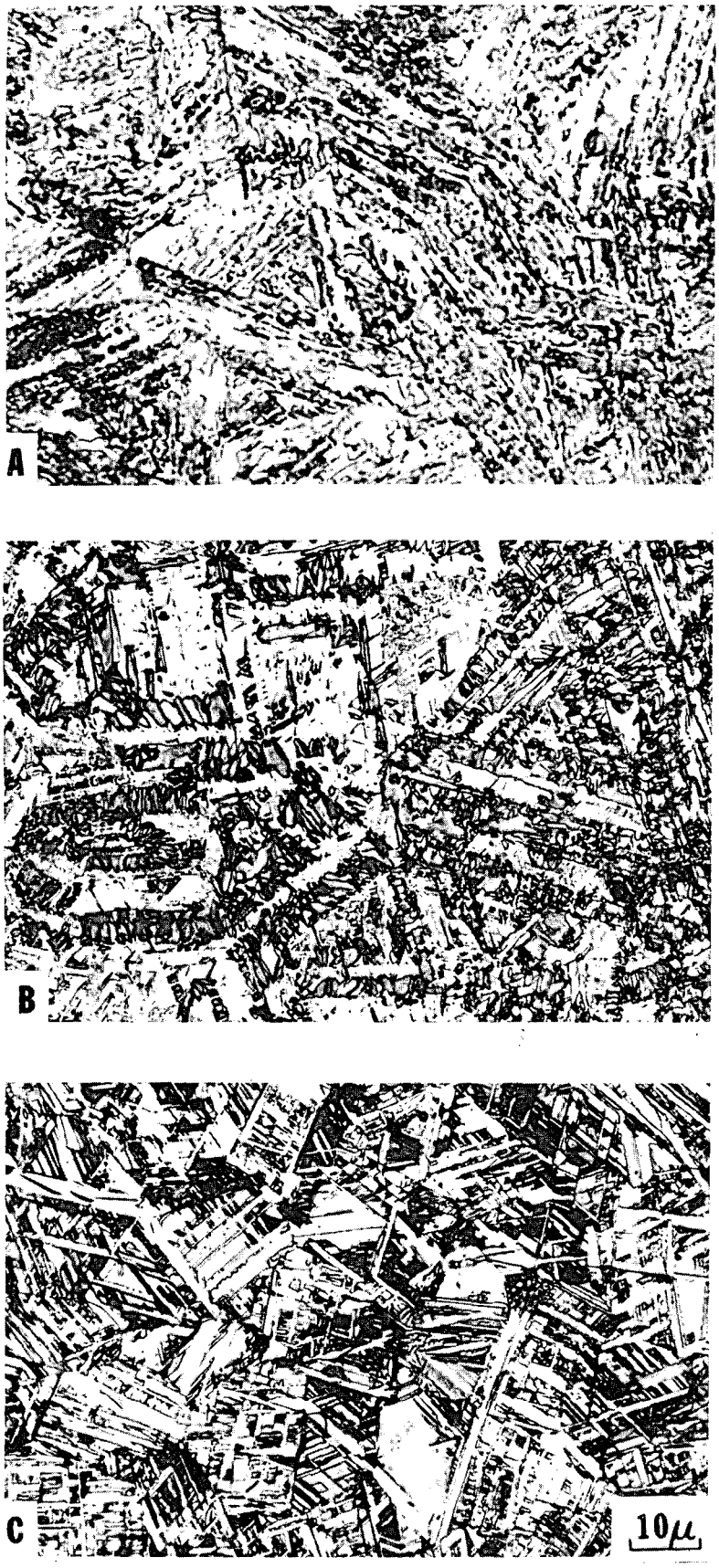

XBB 745-3080

Fig. 2

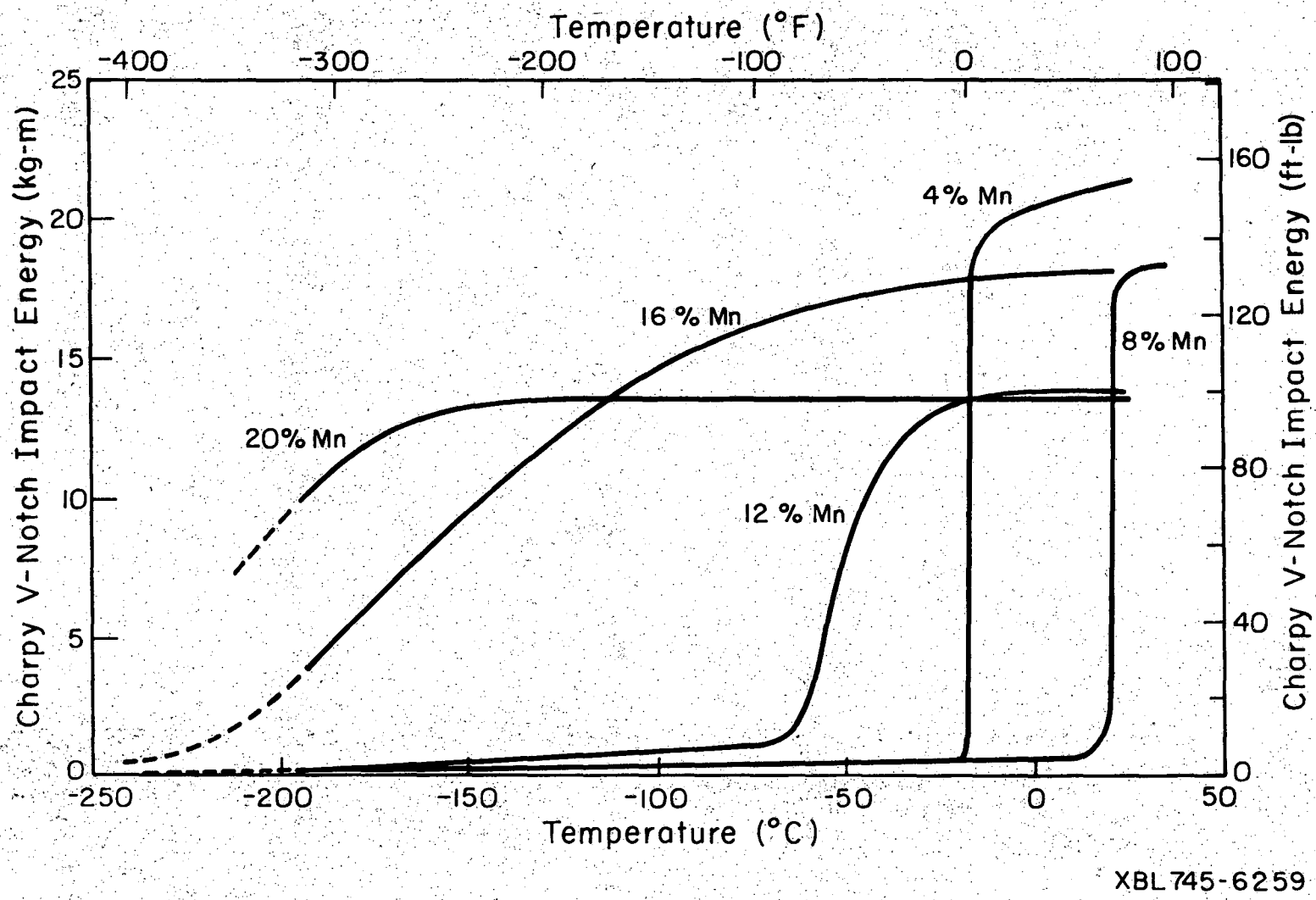
Temperature (°F)
-400
-300
-200
-100
0
100
Charpy V-Notch Impact Energy (kg-m)
25
20
15
10
5
0
Charpy V-Notch Impact Energy (ft-lb)
160
120
80
40
0
4% Mn
16 % Mn
8% Mn
20% Mn
12 % Mn
-250
-200
-150
-100
-50
0
50
Temperature (°C)
XBL 745-6259

Fig. 3

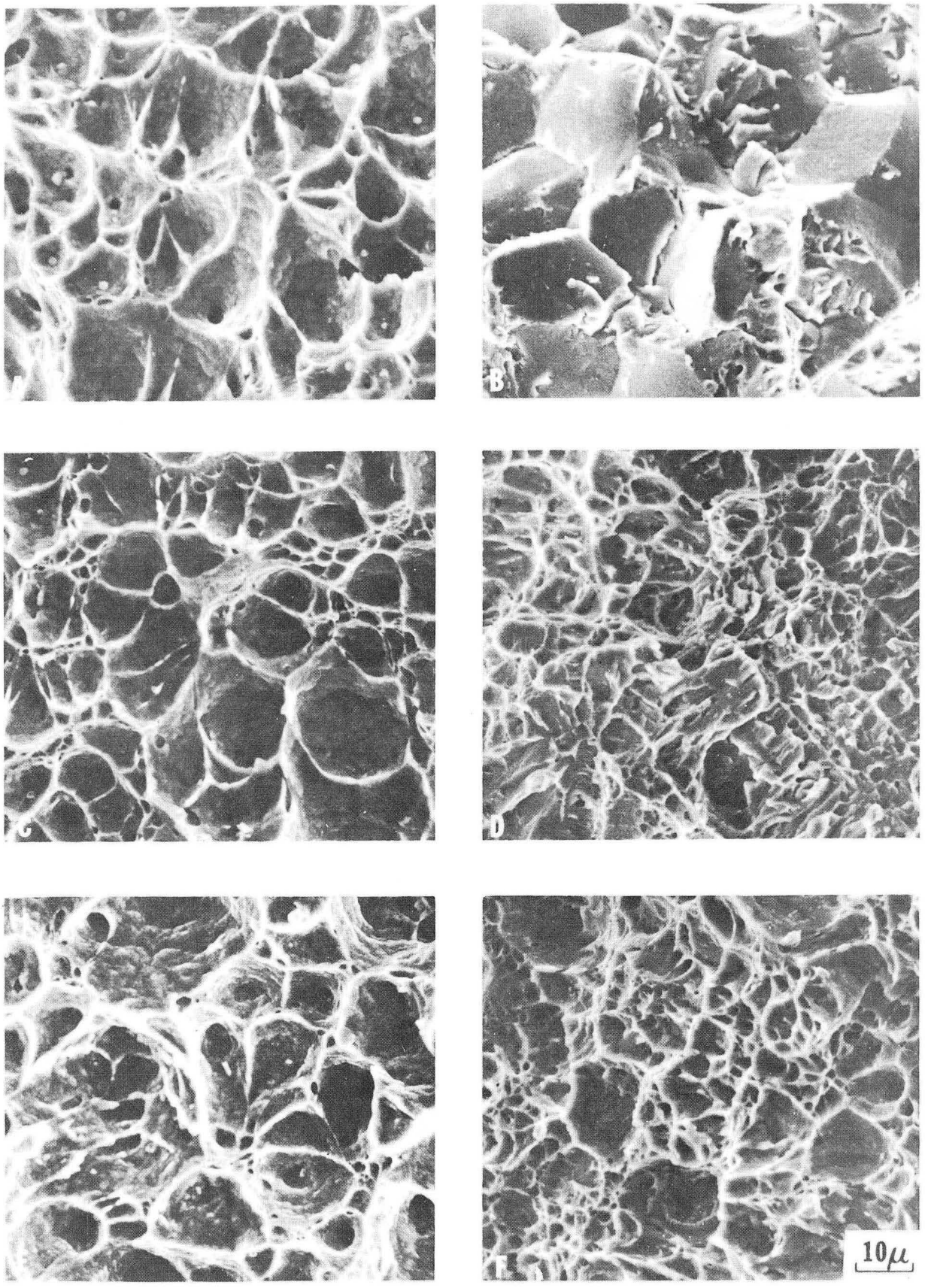

XBB 745-3079

Fig. 4

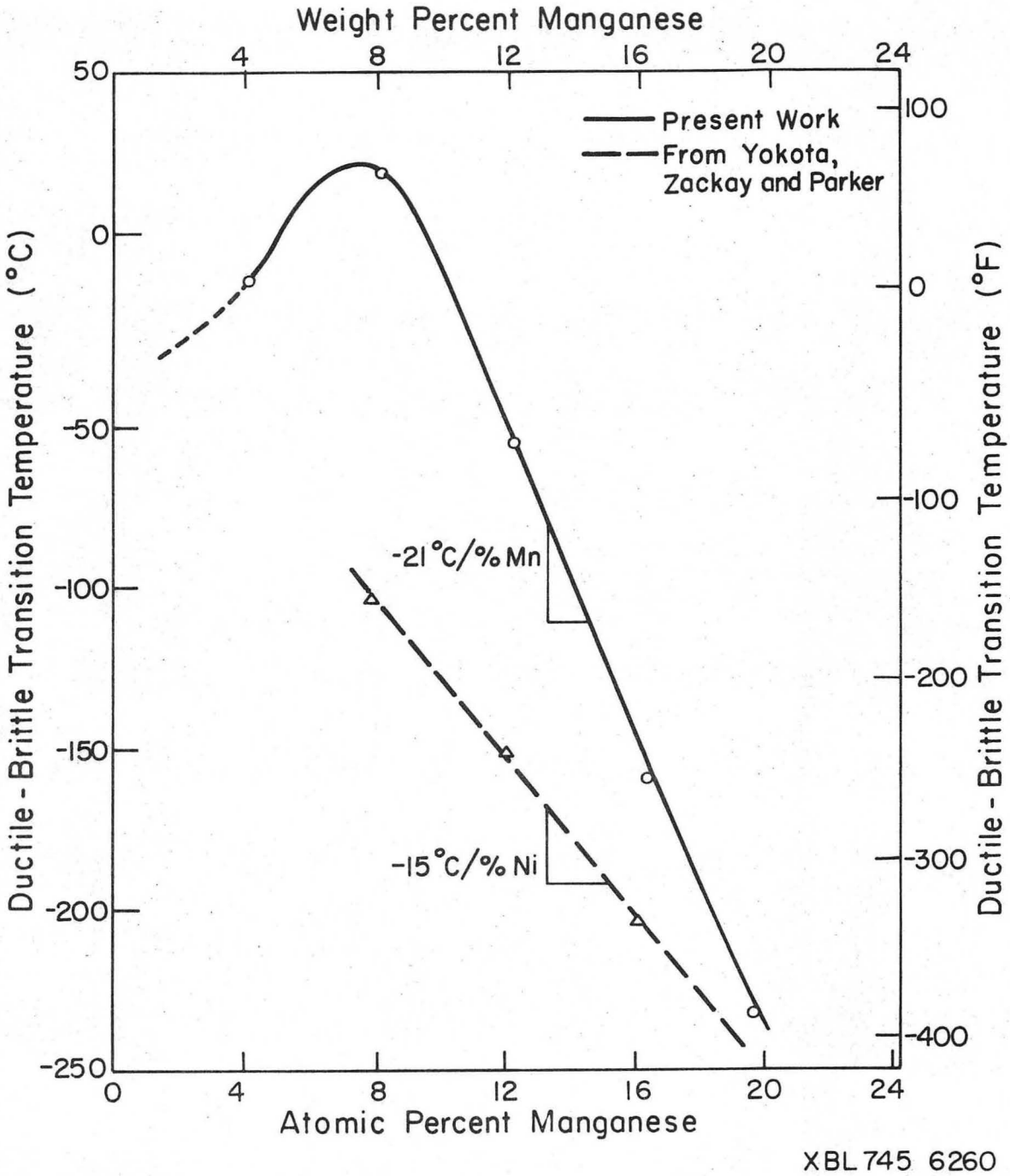
Weight Percent Manganese
4
8
12
16
20
24
50
0
-50
-100
-150
-200
-250
100
0
-100
-200
-300
-400
Present Work
From Yokota, Zackay and Parker
-21 °C/% Mn
-15 °C/% Ni
Ductile - Brittle Transition Temperature (°C)
Ductile - Brittle Transition Temperature (°F)
0
4
8
12
16
20
24
Atomic Percent Manganese
XBL 745 6260

Fig. 5

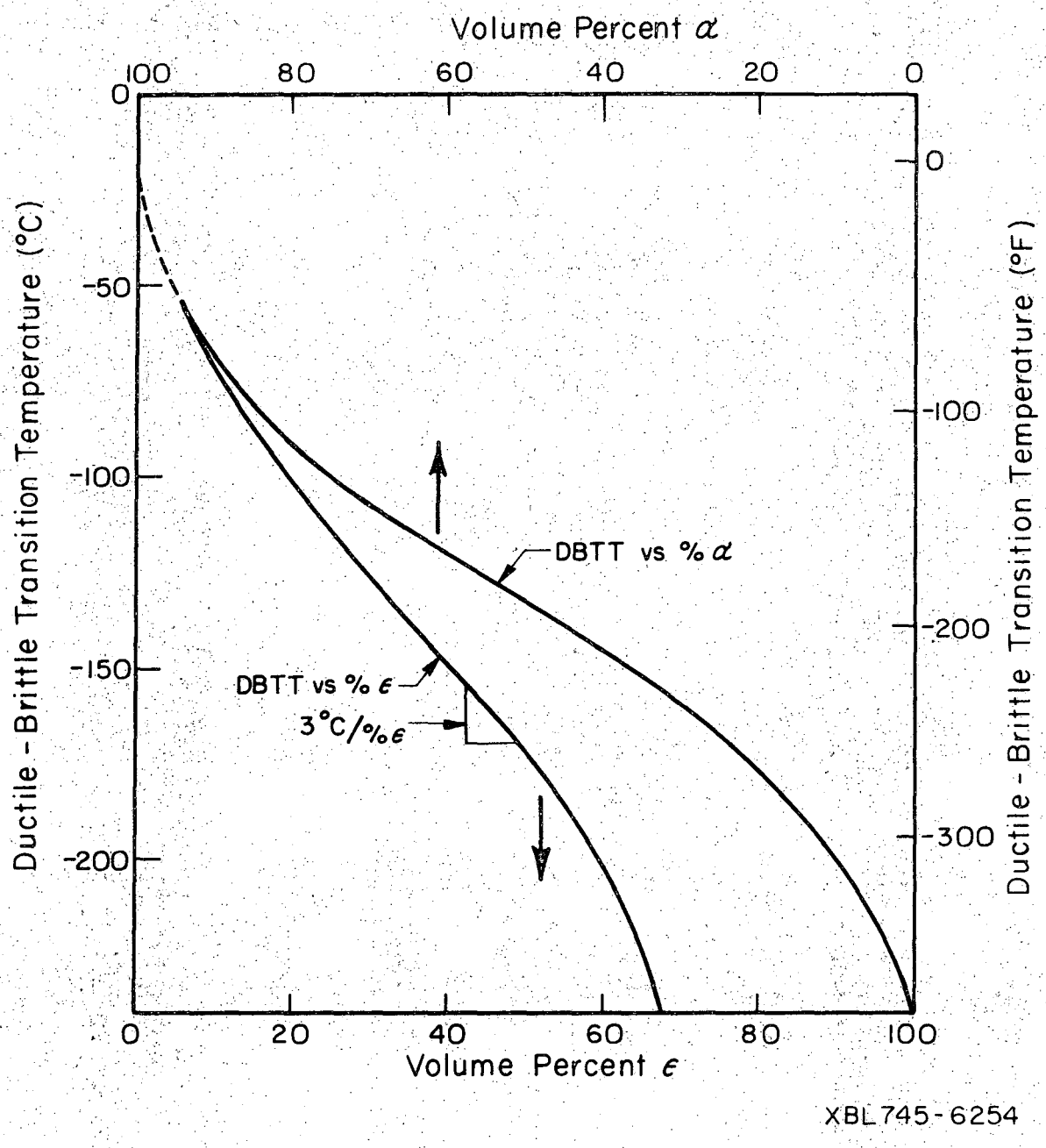
Volume Percent α
100
80
60
40
20
0
0
-50
-100
-150
-200
Ductile - Brittle Transition Temperature (°C)
0
-100
-200
-300
Ductile - Brittle Transition Temperature (°F)
DBTT vs % α
DBTT vs % ε
3°C/% ε
0
20
40
60
80
100
Volume Percent ε
XBL745-6254

Fig. 6

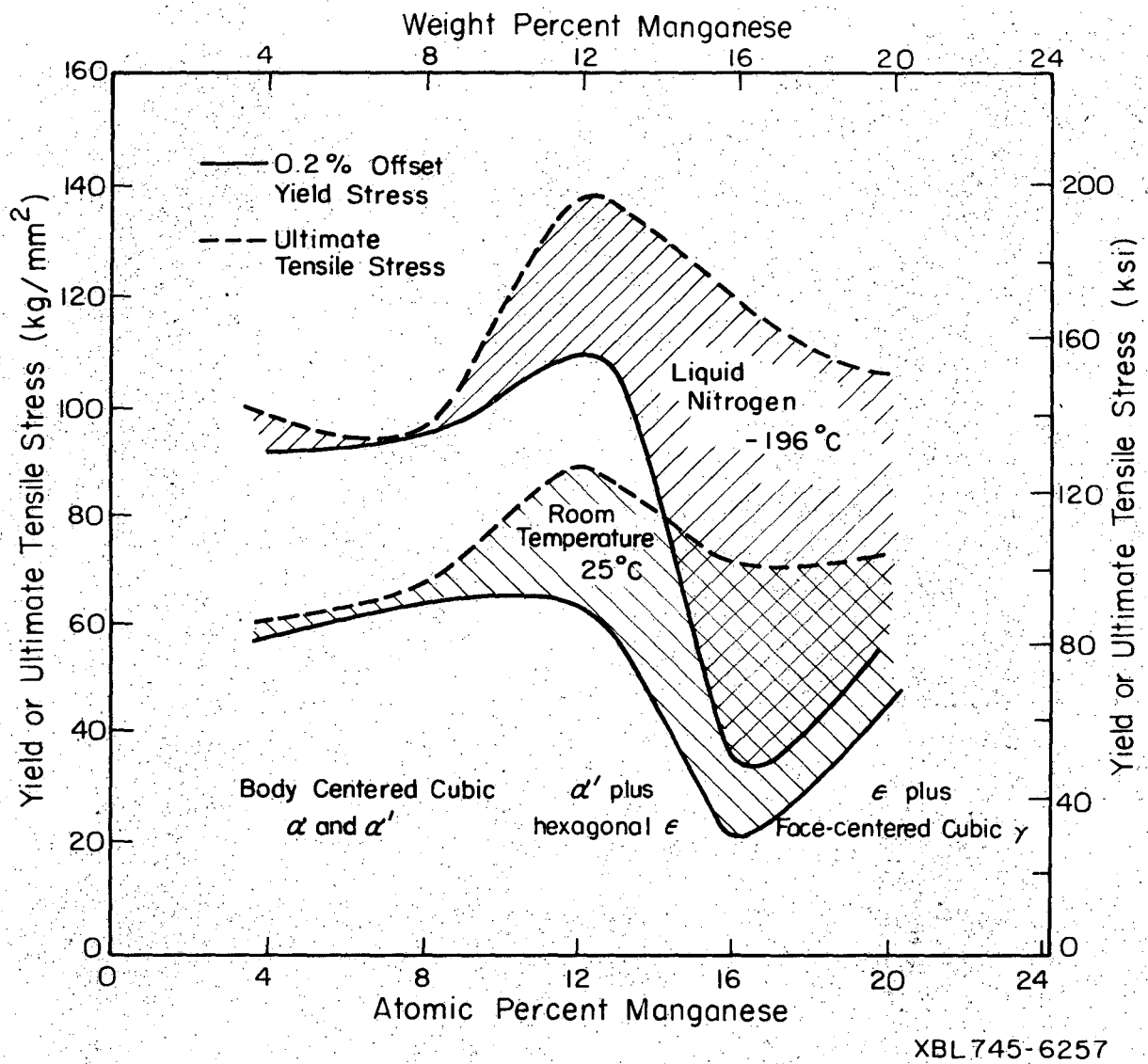
Weight Percent Manganese
4
8
12
16
20
24
160
140
120
100
80
60
40
20
0
Yield or Ultimate Tensile Stress (kg/mm²)
0.2% Offset Yield Stress
Ultimate Tensile Stress
Liquid Nitrogen -196 °C
Room Temperature 25°C
Body Centered Cubic α and α'
α' plus hexagonal ε
ε plus Face-centered Cubic γ
200
160
120
80
40
0
Yield or Ultimate Tensile Stress (ksi)
0
4
8
12
16
20
24
Atomic Percent Manganese
XBL745-6257

Fig. 7

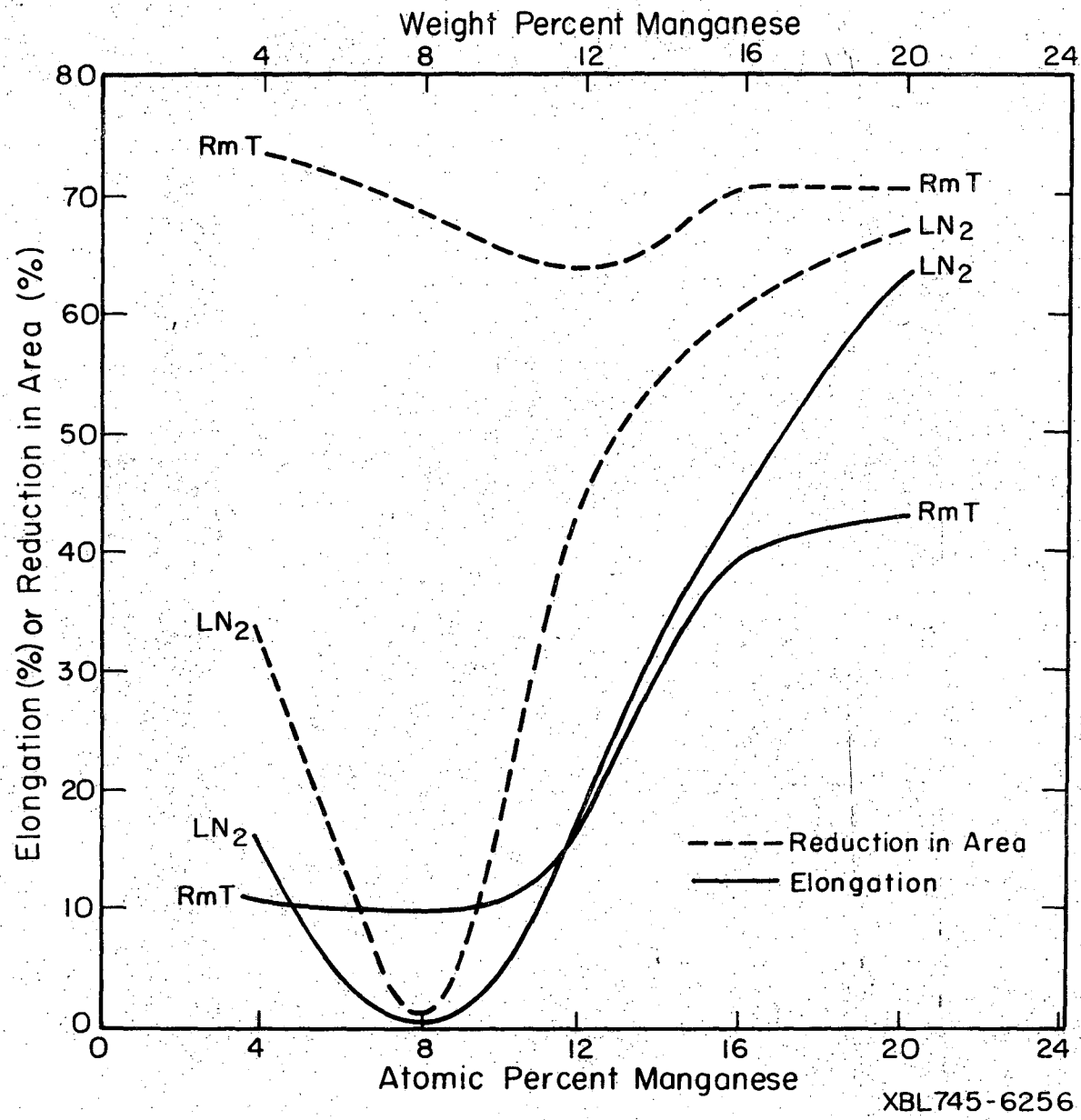
Weight Percent Manganese
4
8
12
16
20
24
80
70
60
50
40
30
20
10
0
Elongation (%) or Reduction in Area (%)
RmT
RmT
LN2
LN2
RmT
LN2
LN2
RmT
Reduction in Area
Elongation
0
4
8
12
16
20
24
Atomic Percent Manganese
XBL745-6256

Fig. 8

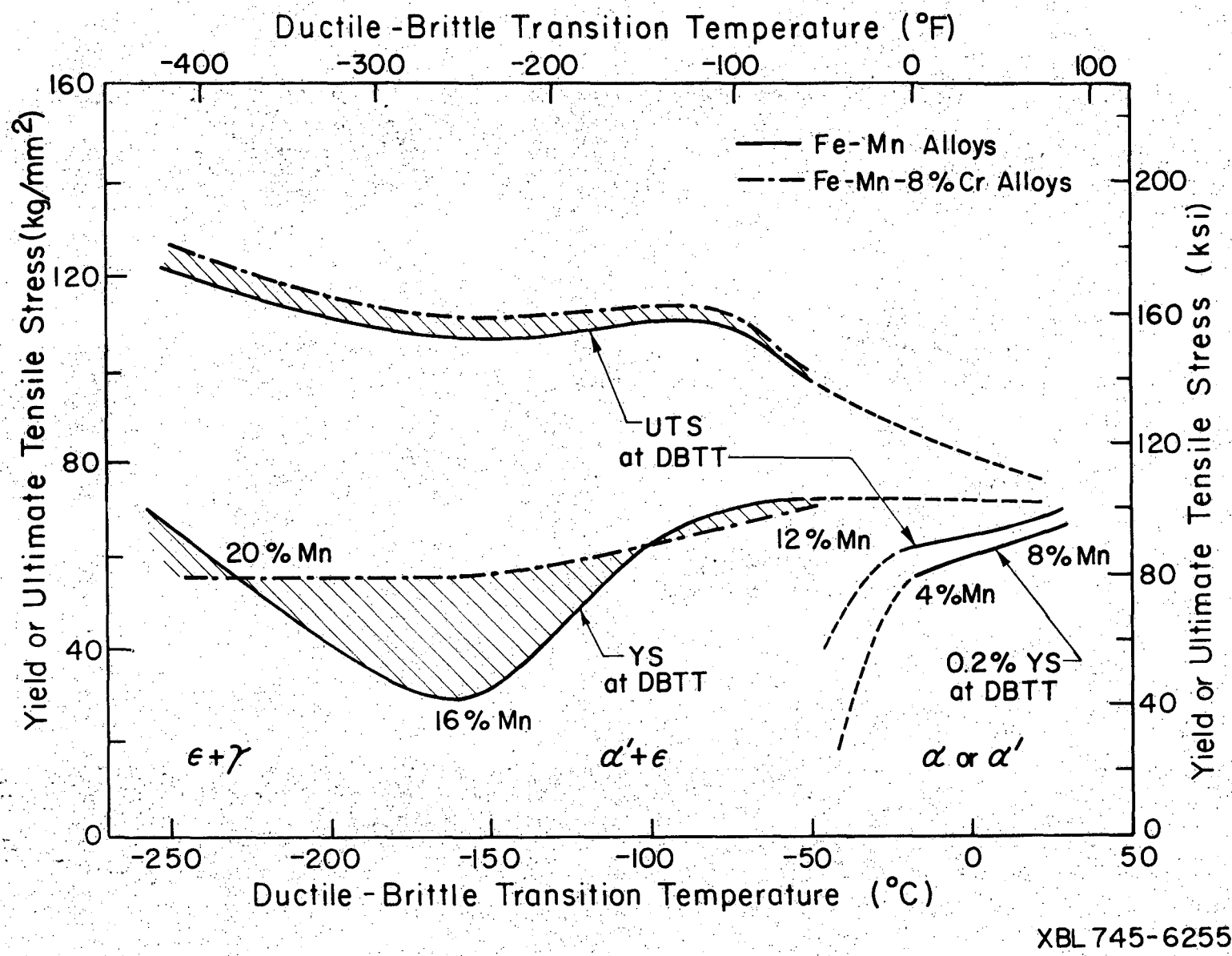
Ductile-Brittle Transition Temperature (°F)
-400
-300
-200
-100
0
100
Fe-Mn Alloys
Fe-Mn-8% Cr Alloys
UTS
at DBTT
20% Mn
12% Mn
8% Mn
4% Mn
YS
at DBTT
0.2% YS
at DBTT
16% Mn
ε+γ
α'+ε
α or α'
Yield or Ultimate Tensile Stress (kg/mm²)
Yield or Ultimate Tensile Stress (ksi)
160
120
80
40
0
200
160
120
80
40
0
-250
-200
-150
-100
-50
0
50
Ductile-Brittle Transition Temperature (°C)
XBL 745-6255

Fig. 9

LEGAL NOTICE

This report was prepared as an account of work sponsored by the United States Government. Neither the United States nor the United States Atomic Energy Commission, nor any of their employees, nor any of their contractors, subcontractors, or their employees, makes any warranty, express or implied, or assumes any legal liability or responsibility for the accuracy, completeness or usefulness of any information, apparatus, product or process disclosed, or represents that its use would not infringe privately owned rights.

TECHNICAL INFORMATION DIVISION
LAWRENCE BERKELEY LABORATORY
UNIVERSITY OF CALIFORNIA
BERKELEY, CALIFORNIA 94720